

Nonintrusive Monitoring for Shipboard Fault Detection

Joshua C. Nation, Andre Aboulian, Daisy Green,
Peter Lindahl, John Donnal, and Steven B. Leeb
Massachusetts Institute of Technology
Cambridge, MA 02139

Lt. Greg Bredariol and Lt. Kevin Stevens
U.S. Coast Guard
& Massachusetts Institute of Technology
Cambridge, MA 02139

Abstract—This paper presents a case study applying nonintrusive load monitoring (NILM) for fault detection and isolation (FDI) of automated shipboard systems. A NILM system installed on an engine room subpanel of U.S. Coast Guard (USCG) Cutter SPENCER collected aggregated power consumption data for ten automated systems. A correlation-based transient identifier is used to disaggregate this data, identifying specific automated load events, including on/off events of the gray water disposal pump. A two-parameter model is calculated from these events and used for fault detection. Data collected during two operational periods of the SPENCER demonstrate the effectiveness of this model in identifying a pump sensor fault previously undetected by the crew. Early identification of such malfunctions prevents costly wear on the gray water disposal system pumps and avoids eventual catastrophic failure.

Keywords—Nonintrusive load monitoring, fault detection and isolation, microgrid, machine diagnostics, condition-based maintenance.

I. INTRODUCTION

New designs for maritime assets, including naval, coast guard, and commercial vessels, are trending toward “optimally” manned crews that are significantly smaller than legacy crew sizes. These reductions in crew size decrease costs, but with increased autonomy, vessels require more robust and reliable sensing to ensure healthy operation of key mechanical and electrical systems [1].

Shipboard power systems are microgrids that present unique prospects for information gathering and control. Opportunities for demonstrating distributed power factor correction, critical load diagnostics, and energy scorekeeping are all immediate on these “islanded” power distribution systems. This trinity represents important avenues for real-time control, automation of ship operation, and informed prognostics and diagnostics for critical ship systems. With distributed power factor correction, it may be possible to incorporate many loads that are essentially transparent to the user, offering greater flexibility in load flow on the network. Critical load diagnostics can provide essential feedback for recognizing and ameliorating energy wasters. HVAC systems, for example, operating under closed-loop feedback control, will continue operating at poor efficiency, e.g., with low levels of refrigerant, with no obvious impact on occupant comfort. Electrical diagnostics can provide essential indications of waste before pathologies become severe. Finally, energy scorekeeping can

provide feedback to operators for enabling cooperative load control. An inexpensive system for energy scorekeeping can provide a detailed breakdown of energy consumption by time and device.

To realize these opportunities, we seek to utilize modern computational tools to our best advantage to track and troubleshoot patterns of energy and utility consumption for critical shipboard loads. Computational power and data transmission capabilities for commercial monitoring and control systems have outpaced our ability to put the right sensors in the right places. Obtaining actionable information in this scenario often requires the proper installation, maintenance, and interpretation of a vast collection of devices—a daunting proposition even if the sensors are mass-produced and individually inexpensive. Alternatively, our approach is to collect fine-grain information from a central point in the electrical system and then leverage increasingly inexpensive computational capabilities to monitor loads.

To accomplish this, we have developed the Nonintrusive Load Monitor (NILM), a comprehensive system for measuring, storing, and interpreting electrical data. The NILM serves as a unique platform for fault detection and isolation (FDI) that is low-cost and easy to install, making it especially suitable for automated vessels with lean crew sizes. This paper demonstrates the use of a NILM installed aboard USCG Famous-Class Cutter SPENCER, where our platform monitored ten mission-critical loads from an engine-room subpanel. The NILM successfully detected a sensor failure in the gray water disposal system. This fault was present during “at sea” operation and was undetected by existing monitoring devices or technicians.

II. LOAD MONITORING AND ANALYSIS

A. The Nonintrusive Load Monitor (NILM)

The Nonintrusive Load Monitor (NILM) is a platform for monitoring electromechanical systems that is practical for widespread application [2], [3], [4]. Fig. 1 gives an overview of its operation. The NILM system monitors aggregate power demand from a central point in a power distribution network. The NILM Meter provides the electrical interface to the power system through a set of LEM LF 305-S current transducers and LEM LV25-P voltage transducers. It rapidly samples (8 kHz) these sensors via an onboard data acquisition (DAQ) device and streams these readings to the NILM software, where they are processed and stored.

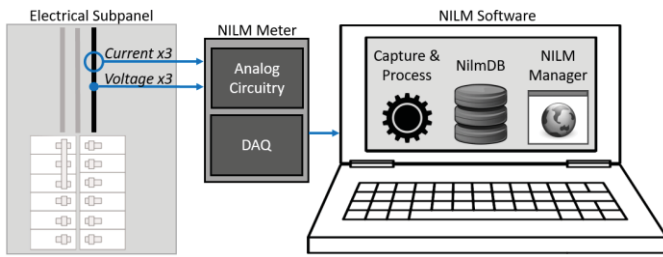


Fig. 2. Overview of the Nonintrusive Load Monitor platform. The NILM Meter measures the 3-phase voltages and currents into a central electrical panel. The software suite processes these readings, and the results are stored alongside the raw data in the NilmDB database. NILM Manager provides a web-based graphical interface for data visualization and analysis from remote locations.

The NILM software suite runs on inexpensive x86 computer hardware. As the capturing utility consumes readings from the NILM Meter, it continuously calculates spectral power envelopes, executes custom user algorithms, and stores the results in the NilmDB database. The spectral power envelopes are computed using the sinefit spectral envelope preprocessor described in [5], effectively converting the high-frequency current and voltage data into fundamental and harmonic components of real and reactive power at 60 Hz intervals. Data is stored locally by the NILM using a custom, network-enabled database, NilmDB [6]. This high-speed time-series database enables efficient storage, retrieval, and processing of the electrical measurements and other information that can be collected from virtually any sensor with a digital interface. Finally, NILM Manager provides a web-based graphical interface for data visualization and analysis from remote locations [7]. NILM Manager includes a transient identification tool, Trainola, which uses a correlation metric to match transients in the power streams to user-identified example transients [2], [6].

This NILM system architecture provides an efficient way to manage large amounts of electrical data. NilmDB can provide a view of load operation over hours, weeks, or months, all dynamically resampled to provide a constant small internet packet for any given request, minimizing bandwidth requirements. The capabilities of the local monitor can be altered or enhanced with short uploads of flexible text-based Python code, enabling on-the-fly modifications of analysis methods and capabilities. This approach is used to inexpensively and quickly develop new load models based on harmonic content, load transient shape, operating schedule, and many other sophisticated parameters not normally considered for load modeling and stability assessment.

Automated computer processing of collected data allows for disaggregation and characterization of system-level transient events created by each load as they change state, e.g. a pump turn-on event. This disaggregated load information is used for tracking equipment operation, energy management and scorekeeping, and fault detection and isolation (FDI).

B. Fault Detection from Operating Statistics

NILM Manager can remotely export files containing timestamps of identified turn-on and turn-off events. It can also accept custom Python scripts to execute over stored electrical data. This is particularly relevant for FDI analysis of systems operating under closed-loop control. These systems are ubiquitous on the SPENCER and typically used to regulate some environmental or operating set point, such as the temperature of the diesel engine lube oil or the water level of the gray water storage tank.

Despite its benefits, closed-loop control can mask underlying electromechanical failures [8]. Without perceivable changes to the environmental or operating set point, subtle problems that do not result in complete system failure often remain undetected. These problems increase energy consumption and impose excessive wear on electromechanical systems as the closed loop control operates a system harder and harder to compensate for system pathologies.

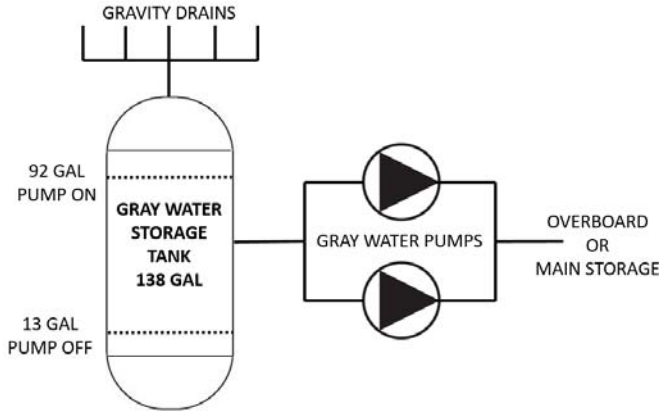
Disaggregated load data obtained by the NILM can be used to hunt down these difficult-to-detect faults, without the installation of expensive sensors or frequent maintenance checks. For the case presented in this paper, two statistical metrics are particularly useful in detecting and identifying a fault: (a) the duration of a particular load event and (b) the period (or equivalently, the frequency) of that load event. While more sophisticated statistical analyses could be performed, these two metrics in combination with an understanding of system operation provide a robust reference frame for diagnosing common system failures.

III. THE SPENCER GRAY WATER SYSTEM

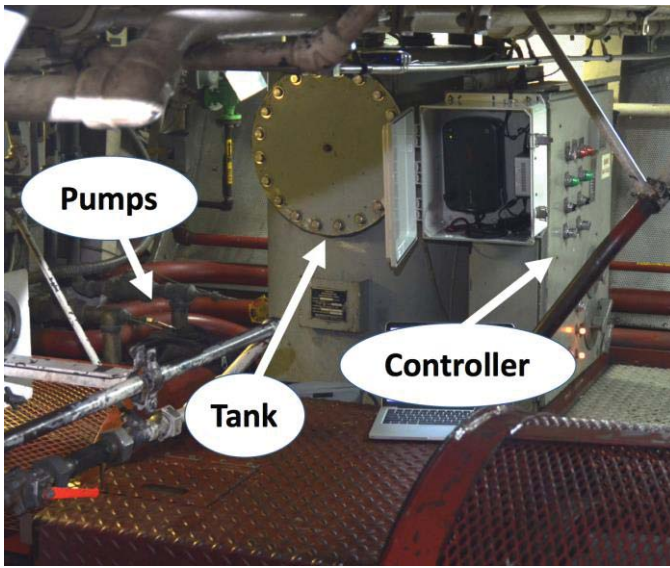
USCG Cutter SPENCER is a 270 ft. (82 m) vessel that hosts a crew of 100 personnel and has an operational tempo of 180 days at sea per annum. This vessel is a prime example of a microgrid, featuring the power generation and distribution equipment required to support missions and sustain crew for months at sea. Multiple NILM systems have been installed at various hierarchical levels of this electrical system. Combined, NILMs are actively monitoring the vessel's 77 induction motors as well as other auxiliary and hospitality loads [2].

The gray water disposal system is a water management network of storage tanks, piping, and pumps. This system is designed to transfer, retain, process, and dispose of the relatively clean water from showers, sinks, washing machines, and other appliances. As depicted in Fig. 3, gravity drains transfer the water from individual receptacles to a 138-gallon (522-liter) storage tank. When the tank is full, water is discharged from the tank and either pumped overboard or transferred to a larger reservoir depending on the vessel's location and applicable pollution regulations.

Two identical pumps (for redundancy) alternate each cycle to discharge the tank. Conductivity sensors detect water levels and provide feedback for pump control. That is, a pump turns on and begins discharging when water reaches the high sensor set point (92-gallon mark), and the pump turns off when water reaches the low sensor set point (13-gallon mark). There is an ~8-second time delay between control signal and pump activation.



(a) Gray Water System Diagram



(b) Photo of Gray Water System

Fig. 3. Diagram (a) and photo (b) of the gray water system aboard USCG Cutter SPENCER. When water reaches the high set point in the tank, a pump begins discharging until the low set point is reached. The two pumps are identical and alternate each cycle. After discharging, the gray water is either pumped overboard or transferred to a larger reservoir on the vessel.

A statistical analysis of the duration and frequency of these discharge pump runs is useful for detecting faults in the gray water system when compared against expected healthy system behavior. The duration of a typical pump run, Δt , depends on the volume of water to discharge, V , and the flow rate of discharge, \dot{Q}_{pump} , i.e.

$$\Delta t = V / \dot{Q}_{pump} \quad (1)$$

From the sensor set points, a pump discharges 79 gallons of gray water each cycle. From estimates of the head pressure in the system and manufacturer-provided pressure-flow rate curves, the flow rate should be approximately 60 gallons per minute. This yields a typical pump duration of ~ 80 seconds (Δt).

Similarly, we can produce a coarse estimation of the time between consecutive pump runs (period) using (2). Here, N is the number of gray water receptacles serviced by the tank (showers, sinks, etc.); ϵ and \dot{q} are the average load factor and average flow rate for the receptacles, respectively. Despite the inherent variations in these parameters based on several usage factors, perhaps most significantly the time of day, a reasonable expected pump-run operation period is ~ 40 minutes (ΔT).

$$\Delta T = V / N\epsilon\dot{q} \quad (2)$$

IV. NILM FDI RESULTS

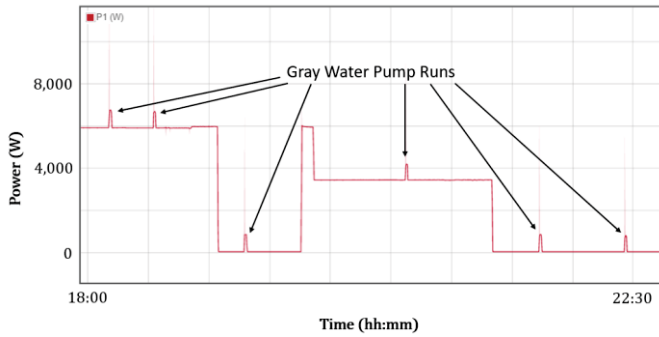
NILM power data was collected aboard USCG Cutter SPENCER during two operational sessions at sea. The gray water pump runs were isolated from the aggregated load data using the Trainola transient identification process [2], [6]. Fig. 4 shows screen captures of the NILM Manager interface. The top plot shows a section of aggregate load data over the course of approximately 4 hours and featuring 6 gray water pump runs. The bottom plot shows an isolated gray water pump run just over 60 seconds in length.

During the first session at sea, both the duration of pump runs and time between pump runs were drastically lower than expected. Following notification of this anomaly, technicians aboard the SPENCER discovered and repaired a failed high set point sensor. During the second session at sea and following this replacement, the gray water system behaved as expected, with the majority of pump run durations lasting 60-90 seconds and the majority of pump run periods (time between pump runs) lasting ~ 1 hour.

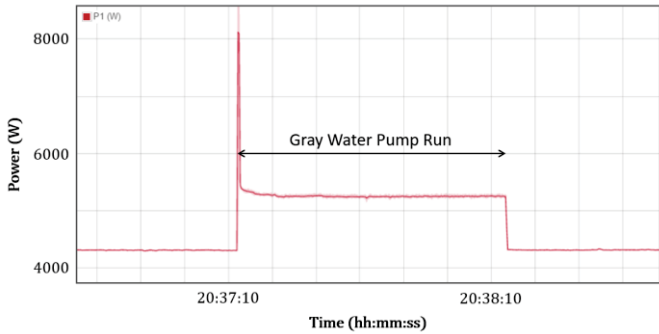
Fig. 5(a) overlays two histograms for pump run duration, one for the healthy system (second operational session) and one for the unhealthy system with sensor failure (first operational session). Similarly, Fig. 5(b) shows the two histograms for pump run period. For both pairs of histograms, there is a significant shift in the histogram distribution. This is most prominent in the histogram comparison of pump run durations.

Further investigation revealed that a sensor failure was present due to a clogged interface between the water and conductivity pads of the sensor. The faulty high sensor thus prematurely sent signals to the pumps to discharge; shortly after, the healthy low sensor sent signals indicating that the tank was empty. This resulted in many short-duration, short-period pump runs.

In this case, early identification of the problem prevented costly wear and tear on the frequently short-cycling pumps and catastrophic failure was avoided due to the NILM. Moreover, the clogged sensors were cleaned in place without a significant interruption to service.

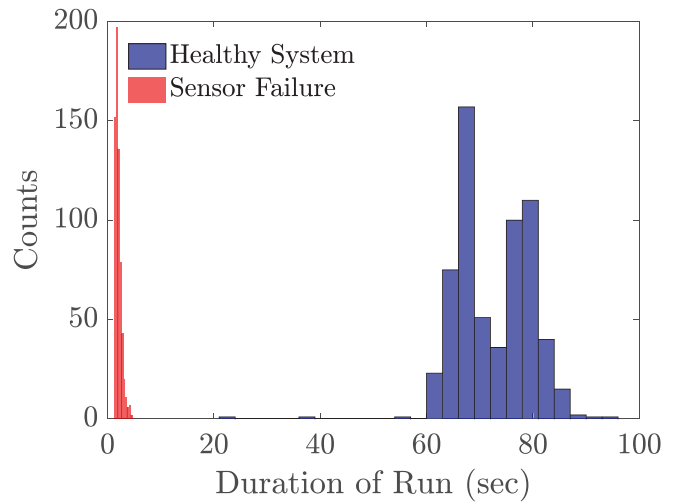


(a) Aggregate Power Data

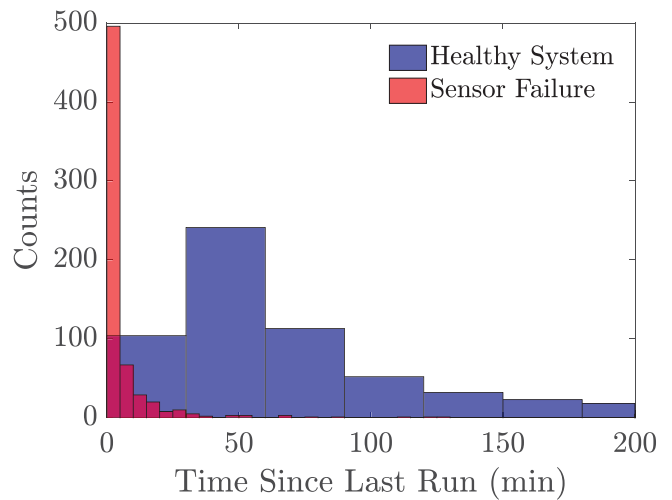


(b) Gray Water Pump Run

Fig. 4. Screen capture of the NILM Manager interface showing NILM aggregate load data (a) and an isolated gray water pump run (b). A built-in transient identification routine allows easy extraction of pump turn-on and turn-off events required for statistical analysis.



(a) Pump Run Duration Histogram

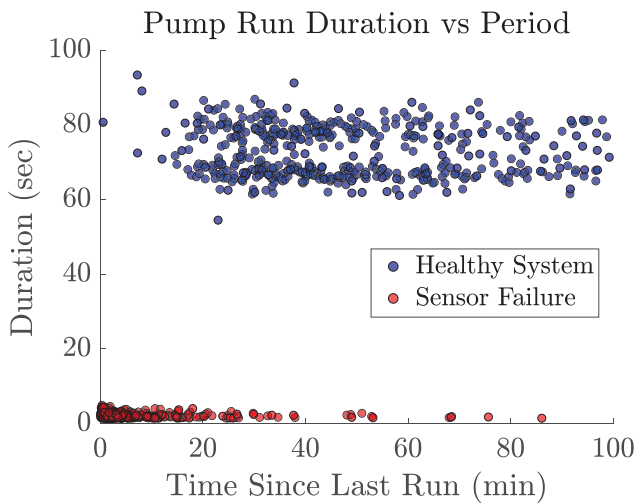


(b) Pump Run Period Histogram

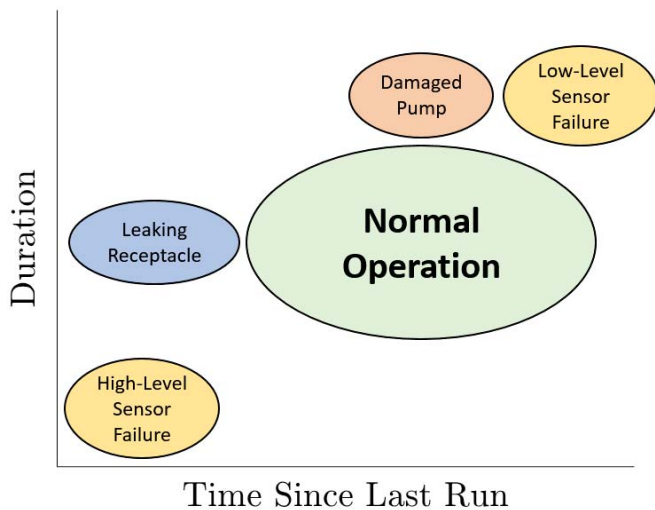
Fig. 5. Histograms of gray water pump run duration (a) and period (b) for both the healthy and unhealthy system data. The healthy and unhealthy data sets were collected during two separate operational sessions at sea. For both the pump run duration and period, the healthy system data aligns with values predicted using basic operational information about the gray water system. In contrast, a drastic shift in both duration and period is evident in the unhealthy data, indicative of a fault (failed sensor).

Fig. 6(a) visualizes each pump run in a 2-D reference frame, where the duration of each pump run is plotted directly against the pump run period. Again, the healthy pump data is shown alongside the unhealthy data with sensor failure. As expected from the histograms, the healthy data is clustered in the top right of the plot (long duration, long period), while the unhealthy data is clustered in the bottom left of the plot (short duration, short period).

Fig. 6(b) indicates expected operation regions in this reference frame corresponding to additional sensor and machinery faults pertaining to the gray water system. For instance, a clogged sensor at the low set point (13-gallon mark) would result in the pump not receiving the “turn-off” signal. In this scenario, the pump would continue draining the tank until it was completely empty, after which dry-running protection would eventually stop the pump and reset the system. This process would likely result in both longer pump durations and longer periods. Other types of failures may primarily affect only duration or period alone. A worn seal or damaged impeller in the pump would decrease the effectiveness of the pump, resulting in longer run durations before the low set point is reached. In contrast, a leaking receptacle (or continuously running appliance) would cause the tank to fill more rapidly, decreasing the pump run period.



(a) Pump Run Duration vs. Period



(b) Pump Run Metrics Translations

Fig. 6. In (a), the pump run duration is plotted directly against the period. For the healthy system, we notice very reasonable values for both, with some variation due to natural usage patterns. By contrast, for the unhealthy system with sensor failure, we see a tight clustering of points at both low duration and low period (though difficult to discern, there are actually >600 data points represented in the unhealthy case). In (b), a graphic is presented that illustrates how various potential faults in the gray water system could manifest on the duration-period plot. This contextualization offers a framework for considering future monitored data and provides a basis for further investigation.

V. CONCLUSION

Closed-loop cycling systems often obscure electromechanical failures and make fault detection difficult.

While operating set points remain constant, system performance gradually degrades and can even eventually result in catastrophic failure. In the best-case scenario, system inefficiency incurs additional cost and wastes resources.

In this paper, we presented a case study demonstrating the effectiveness of nonintrusive load monitoring (NILM) for fault detection and isolation (FDI). Our low-cost, rugged, and easily installed monitoring system collected aggregate power data from a central location aboard USCG Cutter SPENCER. Specific pump load events pertaining to the gray water disposal system were isolated using transient identification. A statistical analysis of two parameters, pump run duration and period, was performed on the load data, and the presence of a fault was immediately detected.

We also considered how our particular sensor failure fits into the context of other potential faults by visualizing these failures on a plot of load duration versus period. Contextualizing potential failures in this way provides a framework for considering future data. As we continue monitoring data aboard SPENCER and on other platforms, we hope to further explore and validate the statistical trends that we have presented here. The ability to not only identify the presence of a failure, but to predict the specific fault, will provide even more benefit to end users.

ACKNOWLEDGMENT

The authors gratefully acknowledge the support of the Office of Naval Research NEPTUNE Program, the MITe-ExxonMobil program, and The Grainger Foundation. The authors also extend their thanks and respect to the incredible men and women of the United States Coast Guard, specifically the crew of USCGC SPENCER, without whom this project would not have been possible, for their professionalism and continued commitment to duty.

REFERENCES

- [1] Lt G. Bredariol (USCG), J. Donnal, P. Lindahl, and S. Leeb, "Automatic watchstander through NILM monitoring," *ASNE Day 2016*, Mar 2016.
- [2] P. Lindahl, J. Donnal, Lt G. Bredariol (USCG), and S. Leeb, "Noncontact sensors and nonintrusive load monitoring (NILM) aboard the USCGC Spencer," *IEEE AUTOTESTCON 2016*, pp. 1-10, 2016.
- [3] G. W. Hart, "Nonintrusive appliance load monitoring," *Proc. IEEE*, vol. 80, no. 12, pp. 1870-1891, Dec 1992.
- [4] G. C. Koutitas and L. Tassiulas, "Low cost disaggregation of smart meter sensor data," *IEEE Sensors Journal*, vol. 16, no. 6, pp. 1665-1673, Mar 2015.
- [5] J. Paris, J. S. Donnal, Z. Remscrim, S. B. Leeb, and S. R. Shaw, "The sinefit spectral envelope preprocessor," *IEEE Sensors Journal*, vol. 14, no. 12, pp. 4385-4394, Dec 2014.
- [6] J. Paris, J. S. Donnal, and S. B. Leeb, "NilmDB: The non-intrusive load monitor database," *IEEE Transactions on Smart Grid*, vol. 5, no. 5, pp. 2459-2467, Sept 2014.
- [7] J. Donnal, J. Paris, and S. B. Leeb, "Energy applications for an energy box," *IEEE Internet of Things Journal*, vol. 3, no. 5, pp. 787-795, Oct 2016.
- [8] J. Paris, J. S. Donnal, R. Cox, and S. Leeb, "Hunting cyclic energy wasters," *IEEE Transactions on Smart Grid*, vol. 5, no. 6, pp. 2777-2786, Nov 2014.